Biochimica et Biophysica Acta, 1144 (1993) 22–32

BBABIO 43856

Each of three positively-charged amino acids in the C-terminal region of yeast mitochondrial ATP synthase subunit 8 is required for assembly

Theo Papakonstantinou, Maria Galanis, Phillip Nagley and Rodney J. Devenish

Department of Biochemistry and Centre for Molecular Biology and Medicine, Monash University, Clayton, Victoria (Australia)

(Received 4 January 1993)

Key words: ATP synthase assembly; Mitochondrion; Mitochondrial import; Allotopic expression; Site-directed mutagenesis; Duplicated targeting sequence; (Yeast)

Each of three conserved positively-charged residues in the C-terminal region of subunit 8 of yeast (*Saccharomyces cerevisiae*) mitochondrial ATP synthase was replaced with isoleucine. The assembly and functional properties of the resulting variants (substituted at Arg-37, Arg-42 and Lys-47) were examined using in-vitro systems to assay import into isolated mitochondria and to monitor assembly into ATP synthase, as well as an in-vivo rescue system using host yeast cells lacking endogenous subunit 8. Each such variant was found to be impaired in assembly in vitro, after import in the form of a chimaeric protein bearing a leader sequence with mitochondrial targeting function. Import precursors bearing a duplicated-leader sequence, engendering enhanced delivery to mitochondria of the passenger variant subunit-8 proteins, enabled assembly of the (Lys-47 → Ile) variant to be detected in vitro but not that of (Arg-37 → Ile) or (Arg-42 → Ile) variants. The respiratory growth of subunit 8-deficient host cells could be rescued with the (Lys-47 → Ile) variant expressed allotopically in the nucleus. Such rescued cells were found to have an enhanced growth rate (comparable to that produced by non-mutagenized parental subunit 8) when delivered to mitochondria with the duplicated-leader sequence, as compared to the single-leader sequence. This confirms that the impediment in the (Lys-47 → Ile) variant lies in the efficiency of its assembly, rather than a functional defect, as such, arising from the loss of that positive charge. In contrast, host cells were unable to be rescued by the (Arg-37 → Ile) and (Arg-42 → Ile) variants, even when they were endowed with the duplicated leader sequence. It is concluded that the positively-charged C-terminal domain of subunit 8, common to fungal and mammalian homologues of this protein, plays a key role in its assembly into mitochondrial ATP synthase.

Introduction

The assembly of multi-subunit protein complexes in biological membranes represents a current focus in molecular cell biology. The proton-translocating mitochondrial ATP synthase (mtATPase) is a multi-subunit enzyme complex that is subdivided into three sectors, designated F_1, F_A and F_0 [1,2]. The F_0 sector is embedded in the inner mitochondrial membrane and constitutes the proton channel of the complex. F_0 is comprised of three hydrophobic proteins, designated subunits 6, 8 and 9 [1]; in yeast, all three are encoded by mitochondrial genes. Subunit 8 (Y8), the focus of this report, is a protein of 48 amino acids [3] encoded in *Saccharomyces cerevisiae* by the mitochondrial *aap1* gene [4]. In contrast to subunits 6 and 9, Y8 has not been assigned a role in proton-channel function as such. It has been shown, however, that Y8 is critical for the assembly of a functional mtATPase [5]; specifically, the presence of Y8 is required for assembly of subunit 6, but not subunit 9, into mtATPase [6].

In our laboratory we have made extensive use of allotopic expression [7] in the study of mitochondrially-encoded proteins, notably Y8. Allotopic expression here involves the functional relocation of a mitochondrial gene to the nucleus and the targeting of the gene product back to the mitochondrion by use of a suitable cleavable N-terminal leader sequence. For Y8, this was achieved using a chemically synthesised gene [8] encoding the 48 residues of Y8 fused to the sequence encoding the 66 amino-acid leader of *Neurospora crassa* mtATPase subunit 9 (N9L) via a 7-amino-acid bridge [9]. This chimaeric precursor protein was designated N9L/Y8–1 [10]. Expression of N9L/Y8–1 in an *aap1 mit*$^-$ yeast strain, lacking endogenous Y8, leads to in-vivo import and assembly of Y8, thus restoring mtATPase function [11]. Following in vitro studies of protein import [9,10] we asked

Correspondence to: R.J. Devenish, Department of Biochemistry, Monash University, Clayton, Victoria 3168, Australia.

whether radiolabelled Y8–1, derived by intramitochondrial processing of imported N9L/Y8–1 and representing Y8 with a 7-amino-acid N-terminal extension, can be assembled into mtATPase complexes of isolated mitochondria. Using an immunoadsorption assay [12] based on an immobilized monoclonal antibody to the F_1-α subunit [13], we showed that the in-vitro assembly of Y8 can be readily achieved, providing the target mitochondria are isolated from yeast cells partially depleted of Y8 [14].

Using these tests, we have begun to probe the function of three highly-conserved positively-charged residues in the C-terminal domain in assembly of Y8 into the mtATPase complex. Initial investigations of the properties of a Y8 variant truncated at Lys-47 [15], denoted N9L/Y8–1(Lys-47 → STP), has suggested an important role for Lys-47 in the assembly process of Y8 [13]. Recognizing that further truncation of Y8, in the variants N9L/Y8–1(Arg-42 → STP) and N9L/Y8–1(Arg-37 → STP), generated Y8 derivatives that were very difficult to import [15], we have adopted the strategy of converting each of the three conserved positively-charged residues to neutral isoleucine residues.

In this study, chimaeric import precursors bearing a tandemly-duplicated N9L leader sequence (N9L-D) have been utilized, as an important adjunct in the analysis of the assembly and function of Y8 variants. Use of N9L-D has been shown to provide a powerful means of conferring enhanced import capability to passenger proteins in vitro [16]. Use of precursors bearing N9L-D leaders fused to modified Y8 passenger proteins has allowed us to determine, with greater resolution, lesions in functional properties of particular Y8 variants [17,18]. In general, the approach involves comparisons of the import and assembly in vitro of a particular Y8 variant fused to N9L or N9L-D, and comparative analyses of cell-growth rates after allotopic expression of the corresponding pairs of chimaeric precursors in vivo [18].

In this paper we describe the properties of three Y8 derivatives, expressed either as single-leader precursors N9L/Y8–1(Lys-47 → Ile), N9L/Y8–1(Arg-42 → Ile) and N9L/Y8–1(Arg-37 → Ile), or in in their corresponding N9L-D configurations. In each case, loss of a C-terminal positive charge from Y8 diminishes the assembly of this subunit, with more severe effects observed for the more proximal residues Arg-37 and Arg-42, compared to the distal residue Lys-47.

Materials and Methods

Plasmids and vectors

The plasmid pUC9 [19] was used as a propagation vector for gene constructs (Fig. 1A), created initially in M13mp19 [20]. The vector pSP64T [21] was used to express N9L/Y8–1 and its variants in vitro (Fig. 1B). The yeast expression vector pPD72 (Fig. 1B) was used to express N9L/Y8–1 and its variants in vivo. The vector pPD72 was constructed by the addition of a sequence block encoding the *ADE1b* selectable marker to expression vector pRJ72 [22]. *ADE1b* designates the *ADE1* gene lacking a single internal *Bam*HI site, prepared as follows: The *ADE1* gene was excised from pLBF101 [11] as a *Kpn*I–*Pst*I segment and cloned into M13mp19. Site-directed in-vitro mutagenesis with oligonucleotide (5′-GGTCAATAGGATACCCTTT TCAGG-3′) was used to introduce a single nucleotide substitution (underlined), such that the *Bam*HI site present in the open reading frame encoding the *ADE1* gene product was lost but the wild-type amino-acid sequence would remain unaltered. This *ADE1b* gene so generated was excised as a 1.9 kb *Xho*I fragment and then ligated into pRJ72, that had been cut with *Sal*I at the unique site located at the 5′-end of the *PGK1* promoter segment, to yield pPD72.

Bacterial strains and manipulations

Escherichia coli K12 strains JM101 [20] and JM109 [23] were used for standard DNA manipulations and maintained according to [24]. The *E. coli* strains CJ236 (*dut*-1, *ung*-1, *thi*-1, *rel*A-1; pCJ105 (Cm^r)) and MV1190 (Δ(*lac*-proAB), *thi*, *sup*E, Δ(sr1-*rec*A)) 306::Tn10 (tet^r) (F′: *tra*D36, *pro*AB *lac* I^{q}Z ΔM15) were used for site-directed in-vitro mutagenesis, and maintained according to the MUTA-GENE^R M13 in-vitro mutagenesis kit handbook (Bio-Rad).

Yeast strains and manipulations

Saccharomyces cerevisiae strain J69–1B (*MAT*α *ade*1 *his*6 (*rho*$^+$)), the derived subunit-8-deficient strain M31 (*aap1 mit*$^-$), and the marker petite strain G5 (*MAT*a *ade*1 *lys*2 *trp*1 (*rho*$^-$)) have been described previously [11]. The genetically-reconstituted strain YGL-1 (M31 expressing the N9L/Y8–1 precursor only under conditions of galactose induction) was as described and grown on medium F [14] containing 2% (v/v) ethanol and 0.5% (w/v) galactose. Growth media for tests of auxotrophic markers, expression of the mutated gene constructs in vivo and retention of *mit*$^-$ genomes in transformant yeast strains, were as described previously [11,14]. Transformation of expression vectors into M31 yeast host cells was according to Klebe et al. [25]. Genetic analyses based on plasmid loss through vegetative segregation during growth on nonselective media, were used to verify that the respiratory growth properties of all respiratory-competent transformant yeast strains were dependent upon the presence of a yeast expression vector, encoding the allotopically-expressed Y8 protein [11]. Confirmation of the identity of mutated gene constructs within transformant yeast strains was carried out as follows: Total yeast DNA was iso-

lated according to Ref. 26 and transformed into competent bacterial JM109 cells [24], selecting for ampicillin resistance. Plasmid DNA bearing the mutant gene construct was prepared essentially as described [24]. The nucleotide sequence of the inserted gene construct was determined by a double-stranded DNA-sequencing protocol, using a T7 sequencing kit (Pharmacia) according to the manufacturer's instructions.

Oligonucleotides

All oligonucleotides were synthesised using an Applied Biosystems Model 380A DNA synthesiser. Parameters for oligonucleotide design included calculation of the free energy (ΔG) of hybridisation of the oligonucleotide to a target gene template cloned in M13mp18 or M13mp19, using the ENERGFIT computer program [8]. The minimum criterion for each oligonucleotide was that its ΔG of hybridisation to the correct region of the template should be at least twice as great as the ΔG value for any nondesired hybridisations. Oligonucleotides synthesised for use as PCR primers were used without purification, but those used for site-directed in-vitro mutagenesis or as sequencing primers were purified as follows: Primers were subjected to polyacrylamide gel electrophoresis and, following UV shadowing [8], the segment of gel containing the oligonucleotide was excised and the oligonucleotide eluted into distilled water by end-over-end agitation overnight at 4°C. Following centrifugation at $5800 \times g$ for 3 min to pellet gel debris, the supernatant was collected and the oligonucleotide concentration determined from the spectrophotometric absorbance at 260 nm. Phosphorylation of the 5'-end of the oligonucleotide for in-vitro mutagenesis was carried out as described [8]. Oligonucleotides homologous to the DNA segment immediately 3' to the cloning site of the vectors M13mp19, pUC9, pPD72 and pSP64T were used for the sequencing of cloned genes.

Site-directed in-vitro mutagenesis

Mutagenesis was carried out using the MUTAGENE^R M13 in-vitro mutagenesis kit (Bio-Rad) according to the supplier's instructions. Templates were single-stranded uracil-containing M13mp19 DNA carrying the target gene encoding N9L/Y8–1. Oligonucleotide primers were (5'-CGCTCATTACAAGATAGAGATGAACAA-3'), (5'-AGAGATGAACAAGATAGAAACGTACAA-3') and (5'-AGAAACGTACAAGATCAAAGATCATTGG-3'), containing base substitutions (underlined), respectively, generating specific amino-acid replacements Lys-47 → Ile, Arg-42 → Ile and Arg-37 → Ile into the Y8 coding sequence (Table I). The oligonucleotides (5'-GAATGGTACCGAATTGAGGC-3') and (5'-GATTGTACGTTTCTAGATTGTTCATC-3') were used to introduce the sequence for two restriction enzyme sites *Kpn*I and *Xba*I, respectively, without alteration to the encoded amino acid sequence of Y8 (Table I). Following each mutagenesis reaction ten plaques were chosen at random and M13 single-stranded DNA was prepared [24]. Screening for the desired mutation was by dideoxynucleotide sequencing [27], using a T7 DNA sequencing kit (Pharmacia), of M13 single-stranded DNA carrying mutated gene cassettes.

Import of proteins into isolated mitochondria and assembly into mtATPase

An in-vitro transcription and translation system was used to produce chimaeric precursor proteins radiolabelled with [^{35}S]methionine [14]. Cell culture and preparation of mitochondria from the yeast strain YGL-1 were as described [13]. Import into mitochondria was carried out and assessed essentially as described [14]. Where required, inactivated mitochondria were prepared by 10 min pretreatment with an inhibitor cocktail (10 μM valinomycin, 10 μg/ml oligomycin and 10 mM KCN). Assays of assembly of Y8–1 and derived variants into mtATPase complexes, involving cholate extraction and an immunoadsorption test using an immobilised monoclonal antibody against the F_1-α subunit, were carried out essentially as described [13].

Uniform cassetting strategy for in-vitro mutagenesis and expression of Y8 variants

A summary of the uniform gene-cassetting strategy is presented here (see also Fig. 1). Details are available upon request from Dr. R.J. Devenish. The genes encoding N9L/Y8–1 and N9L/Y8–2 (a chimaeric protein [10] comprising the 66 amino acids of N9L fused directly to the 48 amino acids of Y8) were converted into DNA cassettes with *Bam*HI and *Not*I sites at the 5' and 3'-termini, respectively. This was done to simplify and facilitate the subcloning of subsequent variant gene constructs into propagation and expression vectors. The Y8-coding region of these cassettes also contained the sequence for two restriction enzyme sites *Kpn*I and *Xba*I (Table I), introduced for later ease of manipulation of mutated Y8 genes. Amplification by polymerase chain reaction (PCR) [15] of the gene encoding N9L/Y8–2 yielded a cassette with a *Bam*HI site at the 5'-end and, sequentially, *Not*I and *Bgl*II sites at the 3'-end. The oligonucleotides utilised for this purpose were Universal Primer (Pharmacia) and (5'-AACTCGAGATCTGCGGCCGCTCATTACAACTTAGAGAG-3'). Following digestion of the purified PCR product with *Bam*HI and *Bgl*II, this cassette was cloned into the unique *Bam*HI site in the M13mp19, pUC9 and pPD72 vectors and the unique *Bgl*II site in the pSP64T vector (thus introducing the appropriately located unique *Not*I site into each vector). Following excision of the N9L/Y8–2 coding region, the

*Bam*HI/*Not*I cassette encoding N9L/Y8–1 was cloned into each of these vectors (as a *Bss*HII/*Not*I cassette in the case of pSP64T) and represents the parent gene template in the various vectors used in this study.

M13 (RF) DNA was used as the primary source of mutagenized double-stranded DNA, specifying N9L/Y8–1 variants. For subcloning genes encoding N9L/Y8–1 variants into the pUC9 holding vector and thence, into the pSP64T expression vector, *Kpn*I/*Not*I cassettes (Fig. 1A,B) were used to replace the corresponding portions of DNA encoding N9L/Y8–1. For transfer into the pPD72 expression vector (Fig. 1B), the *Bam*HI/*Not*I cassettes for all variants derived from the pUC9 holding vector, were used to replace the corresponding segment of DNA encoding N9L/Y8–1.

In general, genes encoding N9L-D/Y8–1 or its variants were constructed by the insertion of a *Bss*HII cassette encoding a second copy of N9L [16] into the unique *Bss*HII site present in each such *Bam*HI/*Not*I cassette, whether already cloned into pPD72 or pSP64T (Fig. 1C). Orientation of the insert was determined by restriction enzyme analysis and confirmed by dideoxynucleotide sequencing (data not shown).

Results

Formation of artificial nuclear gene cassettes encoding subunit 8

The Y8 variants analyzed in this paper were constructed by site-directed mutagenesis of a *Bam*HI/*Not*I cassette containing the N9L/Y8–1 coding sequence (Fig. 1A), into which had been incorporated the restriction enzyme sites *Kpn*I and *Xba*I (Materials and Methods) to facilitate further manipulation of discrete regions of the coding cassette (Fig. 1). In order to probe the assembly and function of the C-terminal domain of Y8, the roles of the three positively-charged residues Lys-47, Arg-42 and Arg-37 were assessed. A set of variants was constructed by in-vitro mutagenesis, in which each of the three positively-charged residues are converted to the neutral residue isoleucine (Ile) (Table I). These variants were subjected to in-vivo assays, utilizing the expression vector pPD72 (Fig. 1B) for Y8 function, and in-vitro assays for Y8 import and assembly, involving the vector pSP64T (Fig. 1B). In addition, further constructs of these Y8 variants were made incorporating a duplicated N9L leader, generating the N9L-D/Y8–1 series (Fig. 1C).

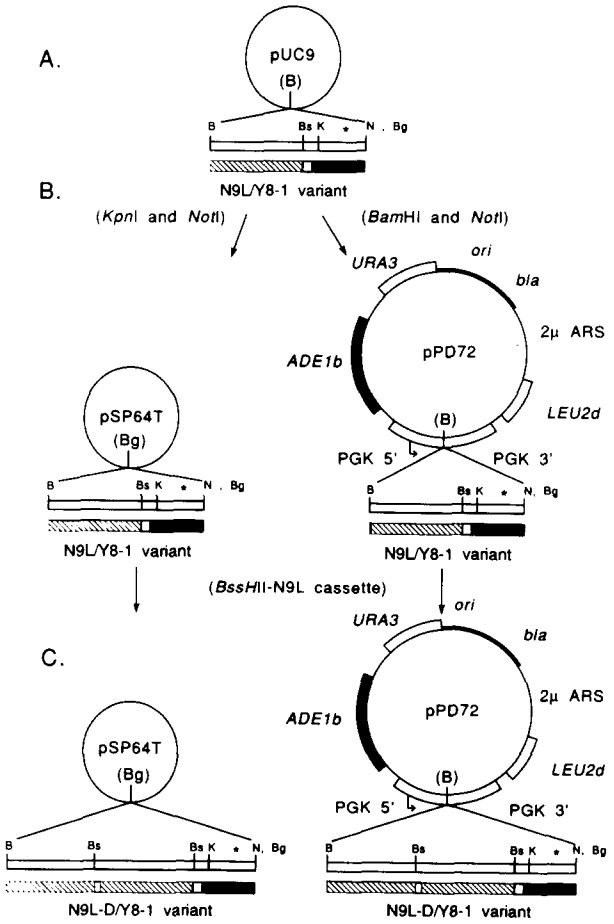

Fig. 1. Subcloning of gene cassettes into expression vectors. The *Bam*HI/*Not*I cassettes encoding N9L/Y8–1 and derived variants cloned in the propagation vector pUC9 (A) were subcloned into in-vitro expression vector pSP64T and in-vivo expression vector pPD72 (B), as *Kpn*I/*Not*I and *Bam*HI/*Not*I cassettes respectively (see Materials and Methods). Tandemly-duplicated N9L leader versions of these genes in pSP64T and pPD72 were also constructed (C). Restriction enzyme sites are as shown (B, *Bam*HI; Bs, *Bss*HII; K, *Kpn*I; N, *Not*I; Bg, *Bgl*II). Additional symbols are: (*), introduced mutation in the sequence encoding Y8; hatched box, *N. crassa* subunit 9 presequence (N9L); open box, bridging sequence consisting of the first five residues of mature subunit 9 sequence plus two serine residues; solid box, Y8 sequence; small open box within the N9L-D segment, a tripeptide formed in the construction of the tandemly-duplicated N9L leader. Concerning the yeast expression vector pPD72, relative positions are shown for the following DNA segments: *E. coli* DNA specifying plasmid replication origin (*ori*) and ampicillin resistance (*bla*); yeast DNA specifying the 2 μm autonomous replication sequence (2μ ARS) and other designated chromosomal genes *URA3, ADE1b* and *LEU2d*, as well as the transcriptional control sequences from the *PGK1* gene. The direction of transcription of *Bam*HI-*Not*I cassettes is in the direction of the arrow from the 5′ promoter segment (5′-PGK) to the 3′ transcription terminator segment (3′-PGK).

Analysis of in-vitro import of N9L/Y8–1 and derived Y8 variants

The in-vitro expression and import behaviour of N9L/Y8–1 generated from the *Bam*HI/*Not*I cassetting system using pSP64T, was equivalent to that observed previously [13]. Thus, the precursor carrying unmodified Y8, N9L/Y8–1 (Fig. 2A, lane 1) was imported by energised mitochondria and processed to Y8–1 (lanes 2–6), which was protected from digestion by the externally added proteinase K (lane 7). No precursor import or processing occurred after incubation with inactivated mitochondria (lane 8), although

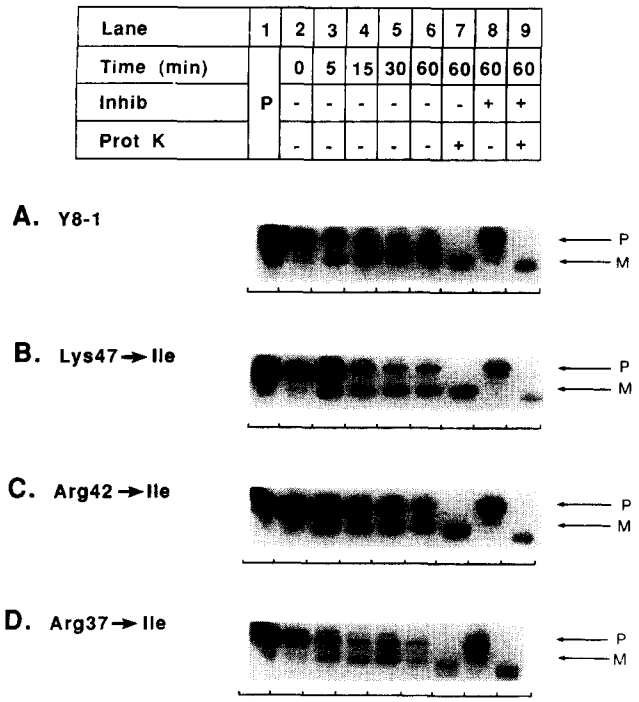

Fig. 2. Import properties of Y8 fusion proteins carrying a single N9L leader. Precursors were incubated with mitochondria isolated from the strain YGL-1. Aliquots of the import mixtures were taken at the times indicated and processed for gel electrophoresis and fluorography. Where indicated, mitochondria were pretreated (Inhib) with an inhibitor cocktail, or treated with proteinase K following the import reaction. Lane 1 contains precursor (P) alone, before addition to mitochondria. Positions on the gels of precursors (P) and the mature processed protein (M) are shown. Panel A, N9L/Y8–1; panel B, N9L/Y8–1(Lys47 → Ile); panel C, N9L/Y8–1(Arg-42 → Ile); panel D, N9L/Y8–1(Arg-37 → Ile). The contents of each lane, in terms of sample treatment, are indicated schematically at the top of the figure.

some radiolabelled protein with slightly higher mobility than Y8–1 remained after treatment with proteinase K (lane 9), which is considered to arise from non-specific embedding of Y8–1 into the outer mitochondrial membrane [9,10]. This proteinase-K-resistant material was previously observed also when radiolabelled Y8 was incubated with isolated mitochondria, either active or inactivated [9].

The set of isoleucine substitution variants were then examined for the ability to be imported into mitochondria in vitro. All precursors were able to be imported (Fig. 2B–D), but to a reduced extent compared to that of the parent N9L/Y8–1 construct (Fig. 2A). The reduction in import did not reflect reduced binding to mitochondrial membranes, as the percentage input of precursor bound to mitochondria was the approximately the same for all four constructs (data not shown). The variants in this study did not display the gross import deficiencies that were observed for the corresponding truncation variants at Arg-42 and Arg-37 [15]. In general, as the ablated positive charge was moved further from the C-terminus of Y8, the import efficiency decreased (compare lanes 2–6 of panels B, C and D) in that the precursor in each case showed a decreasing proportion of the bound precursor to be converted to the mature Y8–1 size product, which was in each case resistant to externally added proteinase K (lane 7 in each panel). The time-dependent diminishing intensity of bands, both precursor and Y8–1 size product, in the case of N9L/Y8–1(Arg-37 → Ile) (Fig. 2D) is reproducible, suggestive of some susceptibility to proteolytic cleavage during the incubation. Finally, in all cases, after incubation with inactivated mitochondria (lane 9), the precursors generated a significant band corresponding to the non-specificallv embedded Y8–1 moiety (see above).

Analysis of in-vitro assembly of N9L / Y8–1 and derived Y8 variants

The ability of Y8–1 and derived variants to assemble into mtATPase complexes in isolated mitochondria, was monitored by exploiting the ability of a monoclonal antibody directed against the F_1-α subunit (linked to Sepharose beads) to capture assembled mtATPase complexes [13]. Target mitochondria isolated from strain YGL-1, partially depleted of endogeneous Y8 by

TABLE I

Sequence of artificial subunit-8 gene variants and predicted amino-acid changes

Subunit-8 variants were expressed in vitro or in vivo as chimaeric precursors carrying either a single leader N9L or the same leader sequence tandemly duplicated (N9L-D). The first A in the initiator methionine (ATG) in the artificial gene encoding Y8 [8] is defined as nucleotide + 1. within codon number 1.

Gene construct	DNA sequence number	Nucleotide change	Codon number	Codon change	Amino-acid change
NAP81-003	+15	T → A	5	GTT → GTA	none [a]
NAP81-003	+123	C → T	41	TCC → TCT	none [b]
NAP81-003-1	+140, +141	A → T, G → C	47	AAG → ATC	Lys → Ile
NAP81-003-2	+125, +126	G → T, A → C	42	AGA → ATC	Arg → Ile
NAP81-003-3	+110, +111	G → T, A → C	37	AGA → ATC	Arg → Ile

[a] *Kpn*I restriction enzyme sequence introduced without alteration of encoded Y8.
[b] *Xba*I restriction enzyme sequence introduced without alteration of encoded Y8.

deliberately regulated allotopic expression in vivo [14], were used for these studies. Partial depletion of Y8 from the inner mitochondrial membrane, has been shown to be required for efficient detection of assembly of imported Y8 into mtATPase [14].

The imported and processed Y8–1 derived from expression of N9L/Y8–1 using the *Bam*HI/*Not*I cassette was readily observed to assemble in vitro (Fig. 3A), as in previous work [13]. Processed Y8–1 (lane 1) was efficiently extracted into a cholate-soluble fraction (lane 2) and immunoadsorbed onto the antibody-coupled Sepharose beads (lane 3). As we have noted previously, some radiolabelled material remains in the post-immunoadsorption supernatant (lane 4) and can also be seen in the cholate-insoluble fraction of the mitochondrial extract (lane 5) [13]. The key visual index of efficient assembly is a greater intensity of material in lane 3 compared to lane 4, as seen in panel A. Further detailed quantitation of the recovery of immunoadsorbed material was impracticable, especially in panels B, C and D. Using this standard assembly assay, all three variants showed no detectable assembly in vitro (lane 3 of Fig. 3B–D). Each variant was shown to be

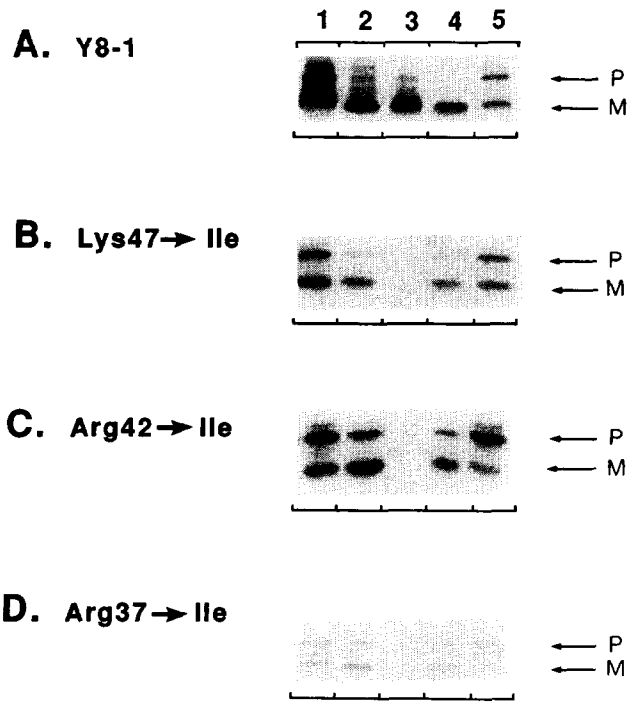

Fig. 3. Assembly properties of Y8 fusion proteins carrying a single N9L leader. Radiolabelled precursors as for Fig. 2 were incubated with mitochondria from YGL-1 under active import conditions. During the assembly assay fractions 1–5 were generated (1, active import mix taken at 60 min; 2, cholate-soluble fraction; 3, immunoadsorbed fraction; 4, post-immunoadsorption supernatant; 5, cholate-insoluble residue) which were analyzed by gel electrophoresis and fluorography. The numbered lanes represented in each fluorogram correspond to the fraction of the same number. The positions of the precursor (P) and the mature processed passenger protein (M) in each case are indicated.

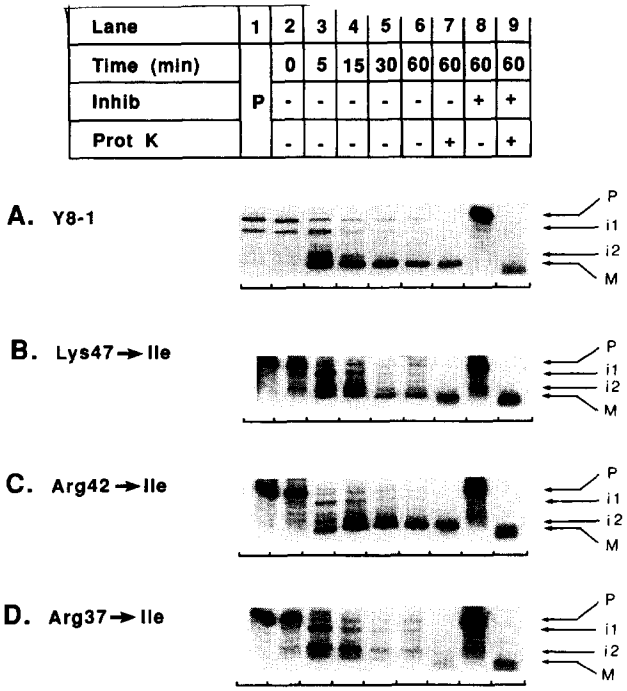

Fig. 4. Import properties of Y8 fusion proteins carrying the tandemly duplicated N9L-D leader sequence. All indications are as for Fig. 2 with the following exceptions. Panel A, N9L-D/Y8–1; panel B, N9L-D/Y8–1(Lys-47 → Ile); panel C, N9L-D/Y8–1(Arg-42 → Ile); panel D, N9L-D/Y8–1(Arg-37 → Ile). The positions are indicated of the precursor (P), processing intermediates (i1 and i2; see text) and the mature processed protein (M).

extractable into the cholate buffer, although the yield of radiolabelled material of Y8–1 size for each variant was generally less than that of Y8–1 itself (compare lanes 2 of panels A to D). Following the immunoadsorption incubation most of the Y8–1 variant material was found either in the supernatant (lane 4) or in the cholate-insoluble fraction (lane 5) but not attached to the antibody-coupled beads (lane 3). These data indicate the primary assembly defect in each of the variants studied, representing ablation of each positive charge in Y8. Note, however, the diminished recovery of the Y8–1(Arg-37 → Ile) variant in all lanes, characteristic of this Y8 variant (see below).

Analysis of in-vitro import and assembly of N9L-D / Y8–1 and derived Y8 variants

A powerful means of enhancing the delivery of passenger proteins to mitochondria is the duplication of the N-terminal leader sequence [16]. This strategy was tested as an approach to extending the range over which impaired assembly properties of particular Y8 variants can be monitored. The remarkable enhancement of import of the parent construct N9L-D/Y8–1, generated from the *Bam*HI/*Not*I cassetting system using pSP64T, is shown in Fig. 4A. This precursor (lane 1) was imported and processed very rapidly by energised mitochondria and generated, through two

processing intermediates i1 and i2, processed Y8–1 almost quantitatively (lanes 2–6). These intermediates i1 and i2 arise from the sequential matrix proteinase cleavage within [28] each of the duplicated N9L leader sequences (but not at the junction between them) and finally at the cleavage site that releases mature Y8–1 [16]. The imported material is resistant to proteinase K (lane 7). Inactive mitochondria show little if any processing of precursor protein (lane 8), but after proteinase K treatment the embedded, trimmed Y8 moiety can be seen (lane 9).

Analysis of the import profiles for the N9L-D/Y8–1(Lys-47 → Ile) and N9L-D/Y8–1(Arg-42 → Ile) precursor variants, indicates a similarly efficient import and processing by energised mitochondria (Fig. 4B and C, lanes 2–6), as for N9L-D/Y8–1. The fully processed Y8–1 derivative is proteinase K-resistant inside mitochondria (Fig. 4B and C, lane 7). For all variants (Fig. 4B–D) the inactive mitochondria bind precursor efficiently (lane 8), yielding an embedded Y8–1 derivative after proteinase K treatment (lane 9).

The N9L-D/Y8–1(Arg-37 → Ile) variant (Fig. 4D, lane 1) differs from the other two variants. Whilst exhibiting a greatly facilitated import of precursor during the first 15 min of incubation (Fig. 4D, lanes 2–4) relative to its single-leader counterpart (Fig. 2D), the N9L-D/Y8–1(Arg-37 → Ile) variant showed considerable instability as a processed product such that material of Y8–1 size was rapidly degraded (Fig. 4D, lanes 5 and 6). In this respect, the susceptibility of Y8–1(Arg-37 → Ile) to proteolytic degradation after import into mitochondria is even greater than that seen for the corresponding single-leader construct (Fig. 2D, lanes 4–6). This instability does not reflect reduced binding to mitochondrial membranes, as all four N9L-D constructs have been found to exhibit a much higher percentage of precursor bound to mitochondria, when compared to their single-leader counterparts (data not shown).

Using the N9L-D constructs, the Y8–1(Lys-47 → Ile) variant was shown to assemble into mtATPase of isolated mitochondria, as well as the parental Y8–1 construct. In both these cases a strong signal of Y8–1 sized material was registered after immunoadsorption (lane 3 of Fig. 5A and B), clearly more intense than the material in the corresponding post-immunoadsorption supernatant (lanes 4). This finding suggests that improved delivery of Y8–1(Lys-47 → Ile) overcomes a kinetic impediment to assembly when a single N9L leader is used, as in N9L/Y8–1(Lys-47 → Ile) (Fig. 3B, lane 3).

In the case of N9L-D/Y8–1(Arg-42 → Ile), the imported Y8–1 variant is assembled only in trace amounts (Fig. 5C, lane 3); there is in this case relatively more material that is cholate soluble but not immunoadsorbed (lane 4). However, processed Y8–1(Arg-42 → Ile) accumulates and remains stable under the improved targeting functions of the duplicated N9L leader (Fig. 4C). We conclude that Y8–1(Arg-42 → Ile) is much more severely impaired in its assembly than Y8–1(Lys-47 → Ile).

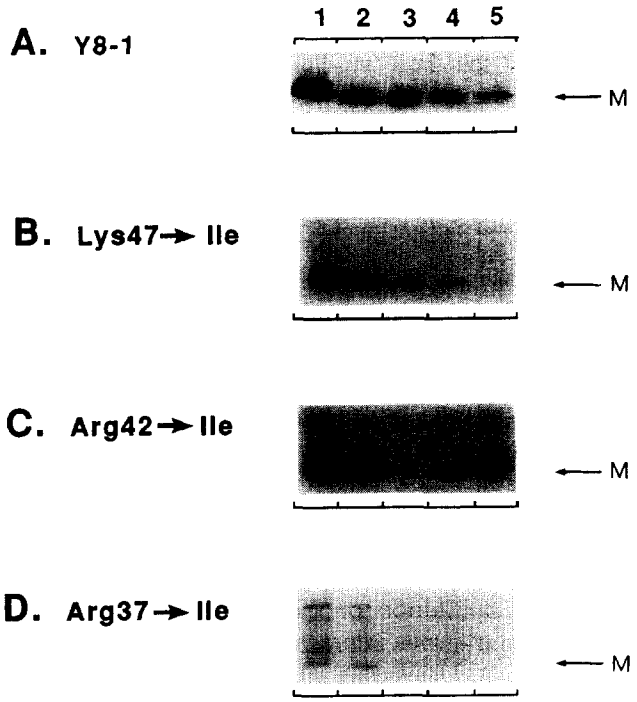

Fig. 5. Assembly properties of Y8 fusion proteins carrying the duplicated N9L-D leader. All indications are as for Fig. 3 with the exception that radiolabelled precursors are as for Fig. 4. The positions are indicated of the mature processed protein (M) in each case.

The situation with the N9L-D/Y8–1(Arg-37 → Ile) variant is more difficult to interpret. In this case, the weak bands in lanes 2–5 of Fig. 5D indicate pronounced loss (perhaps proteolytic) of the processed Y8–1(Arg-37 → Ile) variant, such that very little recovery of Y8–1-sized radiolabelled material is seen in any fraction (Fig. 5D). The faint material in lane 3 of Fig. 5D cannot be regarded as authentic assembly of Y8–1(Arg-37 → Ile), because there is almost equivalent representation of the import precursor and processing intermediates as well as the immunoadsorbed material in this lane. Our failure to observe significant assembly of Y8–1(Arg-37 → Ile) may result from its failure to accumulate properly in mitochondria, although the assembly defect, as such, may be an important feature of this variant.

Expression in vivo of N9L/Y8–1, N9L-D/Y8–1 and derived Y8 variants

In order to test the ability of the Y8–1 variants to function in vivo, the chimaeric precursors bearing single N9L or double N9L-D leader sequences were expressed allotopically in strain M31, lacking endogeneous Y8. DNA segments encoding the relevant pre-

cursors, in the form of *Bam*HI/*Not*I cassettes were inserted into the expression vector pPD72, a multicopy vector with the *PGK1* promoter at the expression site (Fig. 1). The recombinant vectors were tested for their ability to generate rescued transformants of M31, capable of growth on the nonfermentable substrate ethanol at 28°C.

Rescue of M31 was observed with the parental precursor N9L/Y8–1, as previously reported for a related expression vector pLF1 [11]. It was evident from the growth rate of the transformants, exemplified by strain TR-14 in Table II, that delivery of Y8–1 to mitochondria is slightly impaired using this vector. The generation time of TR-14 is 6.39 h, compared to 5.52 h for that of T2–1, strain M31 transformed with pLF1 expressing N9L/Y8–1 [11,13]. Applying Student's *t*-test, this difference is highly significant ($0.01 < P < 0.02$). Further studies suggested some inefficiency in translation of mRNA generated from the expression site (Galanis, M. and Nagley, P., data not shown). It was possible to overcome this relatively inefficient delivery of N9L/Y8–1 to mitochondria expressed from pPD72, by utilizing the double-leader construct N9L-D/Y8–1. The strain YM-2 showed a growth rate corresponding to a 5.65 h generation time, significantly different from that of TR-14 (Table II). This is interpreted to represent the improved targeting and mitochondrial delivery performance that a duplicated-leader sequence can engender in vivo. Precisely how much of the wild-type Y8–1 construct arrives at its correct place in the cells is currently unknown, due to the present lack of an anti-subunit-8 antibody.

Rescue tests with allotopic expression in vivo of the set of isoleucine substitution variants, revealed that only Y8–1(Lys-47 → Ile) was capable of restoring growth on ethanol to the host M31; both single and double-leader constructs of the variants successfully rescued, although generating transformants with significantly different growth rates (see below). Strain TR-17, expressing the single-leader construct of Y8–1(Lys-47 → Ile), showed a significant impairment of growth rate relative to that of strain TR-14 (expressing the corresponding parental Y8–1 construct) at 28°C; TR-17 exhibited a similar growth phenotype at 23 and 36°C, respectively (data not shown), thus arguing against a temperature-sensitive mutation in this yeast strain affecting assembly of mtATPase. This growth impairment was, however, substantially corrected in strain YM-101, expressing the double-leader construct N9L-D/Y8–1(Lys-47 → Ile) (see below). In contrast, neither Y8–1(Arg-42 → Ile) nor Y8–1(Arg-37 → Ile) was able to rescue M31, in either N9L or N9L-D precursor configurations (Table II).

Consideration of the growth rates of TR-17 (7.44 h) and YM-101 (6.06 h), representing single and double-leader precursor configurations of Y8–1(Lys-47 → Ile), respectively, reveals a difference in growth rates that is highly significant (Table II). We interpret this to indicate that the reduced growth rate of TR-17 (relative to TR-14 in the first instance; the difference also being highly significant) is due to the kinetically impaired assembly of this Y8–1 variant that had been manifested in vitro (Fig. 3B). Once assembled, Y8–1(Lys-47 → Ile) is apparently able to function efficiently in the mtATPase. This is manifested by the greatly improved growth rate of YM-101, in which the double leader is considered to enhance delivery of the Y8–1 variant passenger protein and so accelerate its assembly into

TABLE II

Assembly and functional properties of subunit 8 variants in which C-terminal positively-charged residues are individually ablated

For constructs that generated rescued cells, on expression in the vector pPD72, growth rates were determined at 28°C in a supplemented medium containing 2% ethanol (medium E) as the carbon source [14]. Growth rates of rescued cells are indicated as mean generation times, with standard deviation, from three separate experiments. Significance level of differences between growth rates (Student's *t*-test) were as follows: TR-14/TR-17, $0.002 < P < 0.01$; TR-17/YM-101, $0.002 < P < 0.01$; TR-14/YM-2, $0.02 < P < 0.05$; YM-2/YM-101, $0.1 < P < 0.2$.

Transformant strain	Expressed construct	In-vivo rescued cells: generation time (h)	In vitro assembly [a]
A. *Single leader*			
TR-14	N9L/Y8-1	6.39 ± 0.52	strong
TR-17	N9L/Y8-1(Lys47 → Ile)	7.44 ± 0.36	impaired
TR-16	N9L/Y8-1(Arg42 → Ile)	n.d. [b]	n.d.
TR-26	N9L/Y8-1(Arg37 → Ile)	n.d.	n.d.
B. *Double leader*			
YM-2	N9L-D/Y8-1	5.65 ± 0.36	strong
YM-101	N9L-D/Y8-1(Lys47 → Ile)	6.06 ± 0.07	medium
YM-102	N9L-D/Y8-1(Arg42 → Ile)	n.d.	n.d.
YM-103	N9L-D/Y8-1(Arg37 → Ile)	n.d.	n.d.

[a] In-vitro assembly data as summarised from Figs. 3 and 5 (see text).
[b] n.d. = not detectable.

mtATPase. Note that the difference in growth rate between YM-101 and YM-2 (expressing the N9L-D/Y8–1 parent) is not significant (Table II).

Discussion

Assembly and functional aspects of Y8 variants lacking conserved positive charges

Ablation of each conserved positive charge in Y8 leads to a defect in assembly of this subunit into mtATPase. As with the previous experiments carried out using the Y8–1(Lys-47 → STP) truncation variant [13], the Y8–1(Lys-47 → Ile) variant shows negligible assembly in vitro when delivered by a single leader yet generates functional mtATPase when allotopically expressed in the *aap1 mit*$^-$ host M31 in vivo. This suggests, in itself, that Y8 variants lacking the distal positive charge Lys-47 show some impairment in the efficiency of assembly, but with much less impact on function once assembled into mtATPase. The significant new findings in this paper are twofold. First, assembly in vitro of Y8–1(Lys-47 → Ile) can be generated by enhancing the delivery of the passenger protein to mitochondria using the double-leader N9L-D. Similar enhancement in the extent of assembly in vitro was noted for N9L-D/Y8–1(Lys-47 → STP) (data not shown). Second, as amplified below, the rate of growth of M31 cells rescued with N9L-D/Y8–1(Lys-47 → Ile) paralled that of cells rescued with the parent Y8–1 construct, and was significantly greater than of M31 cells rescued with N9L/Y8–1(Lys-47 → Ile). Y8 lacking Lys-47 is minimally impaired functionally. In contrast, Y8 variants lacking the more proximal residues Arg-42 and Arg-37 not only are more severely impaired in assembly compared with their Lys-47 counterpart, but also fail to rescue M31 when endowed with either a single N9L or double N9L-D leader.

Utility of the tandemly-duplicated N9L leader sequence to examine the assembly and functional properties of variants

A particular advantage of studying the enhanced import in vivo of passenger proteins carrying a duplicated leader (N9L-D) [16] is the ability to discriminate between functional and assembly defects in the subunit-8 variant under study. In the case of a Y8 variant manifesting a functional defect, despite the improved delivery into mitochondria using a duplicated leader, little or no enhancement of ATP synthase performance (hence cellular growth rate) could be expected to occur. A Y8 derivative lacking the first three N-terminal residues, derived from processing of the precursors N9L/Y8–2 or N9L-D/Y8–2 [29], is an example of this first type of variant [18]. Using the expression vector pPD72 to express these variant precursors in the *aap1 mit*$^-$ mutant host M31, the growth rates of rescued

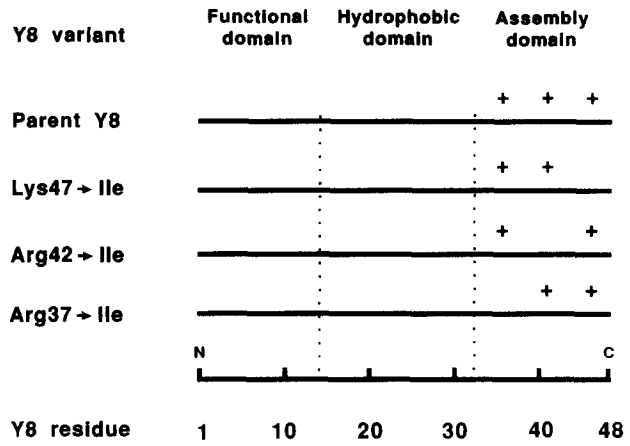

Fig. 6. Schematic illustration of subunit 8 and derived variant proteins lacking individual C-terminal positively-charged residues. Three distinct domains of Y8 with identifiable properties are indicated.

cells were not significantly different when either a N9L or N9L-D construct was expressed. The growth rates were, however, significantly less than that of YM-2 or YM-101 [17]. Further, the imported processed Y8–2 construct shows little impairment in assembly in vitro [13,18]. On the basis of the above results, the N-terminal region of Y8 has been assigned a specific role in bioenergetic function of mtATPase (Fig. 6).

In the case of a variant being affected in the rate of its assembly into mtATPase rather than in its function, the assembly defect should be effectively overcome in vivo by enhanced delivery into mitochondria of the variant using a double-leader precursor construct. This strategy should thus lead to measurable improvement in the growth rate of rescued cells. The results observed for N9L/Y8–1(Lys-47 → Ile) and N9L-D/Y8–1(Lys-47 → Ile) are representative of such behaviour of Y8 variants affected in the rate of assembly. A comparison of the growth rates of TR-17 and YM-101 (Table II) illustrates the ability of duplicated-leader-based delivery to overcome a kinetic block to assembly of Y8–1(Lys-47 → Ile). The improved efficiency of assembly in turn leads to a situation which reflects little direct functional impairment of the final assembled ATP-synthase complexes (compare the very similar growth rates of YM-101 and YM-2, indicated in Table II).

Implications of Y8 domains involved in assembly and the role of the C-terminus

Positively-charged residues at the C-terminus of Y8 represent a highly conserved feature of Y8 homologues in fungi and metazoa [17,30]. We have shown here that ablation of each of these positive charges is deleterious to the assembly properties of Y8. Further, the two positively-charged residues located more towards the central hydrophobic region of Y8 (Fig. 6), seem to be absolutely required for assembly. Note that, after import, Y8–1(Arg-37 → Ile) exhibits an instability that may be related to the effective lengthening the central

hydrophobic domain in this variant. It is possible that this greater suspectibility to proteinase digestion arises from the inability of Y8–1(Arg-37 → Ile) to be properly targeted to its site of assembly into mtATPase. Perhaps Y8–1(Arg-37 → Ile) is arrested in translocation through the membrane and diverted from the regular assembly pathway, entering an intramitochondrial 'dead-end' pathway which may be analogous to that for cytochrome b_2, whose 'dead-end' location is in the matrix [31]. It should be noted that Glick et al. [31] have described an ATP-dependent proteolytic system that degrades polypeptides exposed to the intermembrane space; if the bulk of Y8–1(Arg-37 → Ile) fails to be properly delivered through the inner membrane into the matrix as a result of increased hydrophobicity, such a system could contribute to the proteinase susceptibility of this variant.

An important question to consider is whether the location of the positively-charged residues within Y8 is critical for assembly of this subunit into mtATPase. Analysis of the amino-acid sequence of Y8 homologues in various fungi, for example *Asperigillus nidulans* and *Neurospora crassa*, indicates that additional positively-charged residues are found at residue positions 29 and 34, encroaching on the downstream end of the central hydrophobic region (Fig. 6) of these Y8 homologues [17,30]. We have recently achieved the allotopic expression of the Y8 homologue from *A. nidulans* in yeast strain M31, which leads to functional rescue of these *aap1 mit*$^-$ cells (Straffon, A.F.L. and Devenish, R.J., data not shown). In these cases, it could be asked whether ablation of the C-terminal residues is deleterious for assembly, given the additional charged residues towards the central region of these proteins.

Current experiments are exploring the issue of whether the presence of positively-charged residues located within the central domain of yeast subunit 8 itself, could compensate for the loss of positive charge arising from substitution by isoleucine of the conserved residues at positions 47, 42 or 37. As a prelude to these experiments, we have commenced the insertion of additional positively-charged residues in the central region of Y8. Thus, several variants of Y8 bearing one additional positive charge (such as Gln-29 → Lys, Ile-25 → Lys or Thr-22 → Lys) or even variants bearing two such additional charges (such as Ile-25 → Lys, Gln-29 → Lys) have been constructed and found to rescue efficiently M31 in vivo after allotopic expression [17,18]. These results show the tolerance of Y8 itself for additional positive charges. One interpretation of these findings is that there may not be an absolute requirement for Y8 to be embedded in the membrane, in order to fulfill its function [17,18]. Further, it is possible that all that may be needed for its assembly is a cluster of positive charges towards the C-terminus of Y8, which resides in the matrix [32]. Indeed, a strikingly conserved feature of subunit-8 homologues from fungi and mammals is the positively-charged C-terminal domain, that may be inferred to represent the assembly domain of these proteins (cf., Fig. 6).

Interactions of Y8 with other subunits in the assembly of the F_0 sector

Based on a study of mtATPase assembly in vivo in *mit*$^-$ mutants lacking individual F_0 subunits, the sequential order of assembly of F_0 sector subunits in yeast has been shown to be subunits 9, 8 and 6 [5,6]. It should be noted that, once imported into mitochondria, the allotopically expressed Y8 is assumed to proceed along an assembly route similar to that of subunit 8 in wild-type yeast strains, given the functional rescue of M31 by N9L/Y8–1 and the ability of imported Y8–1 to be immunoadsorbed to mtATPase in vitro.

From the order of assembly of the F_0 subunits, it is considered that Y8 interacts with at least Y9, in its assembly into the mtATPase complex. The C-terminal domain of Y8, required for efficient assembly, must then interact directly or indirectly in some way with Y9 in the assembly pathway. This interaction with the C-terminal domain could be mediated by a chaperonin such as hsp60 [33,34], or the hsp70-related *SSC1* gene product [35]. One other candidate for such interaction is the *ATP10* gene product, a nuclearly encoded protein which has been implicated in having a role in the assembly of the F_0 sector [36]. Residues or domains in subunit 6 (Y6) should also presumably interact with Y8, as assembly of Y6 into mtATPase requires the presence of assembled Y8 in the enzyme complex [6]. Very little information is presently at hand as to whether subunits of the F_A sector interact with Y8 in their assembly into mtATPase, although it has been shown that the assembly of two subunits of this sector (designated P25 and P18) requires the presence of all three F_0 subunits [6]. Assembly of the F_1 sector subunits, on the other hand, does not depend on the presence of Y8, as examination of a *rho*$^\circ$ yeast strain (lacking mitochondrial DNA) has shown that an intact assembled F_1 sector is present, albeit only loosely associated with the inner membrane [37].

In order to further investigate interactions between mtATPase subunits, the N9L-D/Y8–1(Arg-42 → Ile) variant could be utilized, in which import is efficient but assembly is very inefficient. Genetic selection for second-site mutations that promote functional assembly of Y8–1(Arg-42 → Ile) into mtATPase complexes may uncover further mutations in either the Y8 coding sequence or in genes encoding other ATP-synthase subunits. Such experiments have the potential to elucidate key interactions between mtATPase subunits and may offer an exciting new direction for future studies of mtATPase assembly.

Acknowledgements

The work described here was supported by the Australian Research Council. We thank Dr. D. Nero, Dr. R.H.P. Law, Mr. A. Straffon and Mrs. S. Ekkel for assistance.

References

1 Nagley, P. (1988) Trends Genet. 4, 46–52.
2 Cox, G.B., Devenish, R.J., Gibson, F., Howitt, S.M. and Nagley, P. (1992) in Molecular mechanisms in Bioenergetics (Ernster, L., ed.), pp. 283–315, Elsevier, Amsterdam.
3 Velours, J., Esparza, M., Hoppe, J., Sebald, W. and Guerin, B. (1984) EMBO J. 3, 207–212.
4 Macreadie, I.G., Novitski, C.E., Maxwell, R.J., John, U.P., Ooi, B.G., McMullen, G.L., Linnane, A.W. and Nagley, P. (1983) Nucleic Acids Res. 11, 4435–4451.
5 Linnane, A.W., Lukins, H.B., Nagley, P., Marzuki, S., Hadikusumo, R.G. Jean-Francois, M.J.B., John, U.P., Ooi, B.G., Watkins, L., Wilson, T.A., Wright J. and Meltzer, S. (1985) in Achievements and Perspectives of Mitochondrial Research, Bioenergetics Vol. I (Quagliariello, E., Slater, E.C., Palimieri, F., Saccone, C. and Kroon, A.M., eds.), pp. 211–222, Elsevier, Amsterdam.
6 Hadikusumo, R.G., Meltzer, S., Choo, W.M., Jean-Francois, M.J.B, Linnane, A.W. and Marzuki, S. (1988) Biochim. Biophys. Acta 933, 212–222.
7 Nagley, P. and Devenish, R.J. (1989) Trends Biochem. Sci. 14, 31–35.
8 Gearing, D.P., McMullen, G.L. and Nagley, P. (1985) Biochem. Int. 10, 907–915.
9 Gearing, D.P. and Nagley, P. (1986) EMBO J. 5, 3651–3655.
10 Law, R.H.P., Farrell, L.B., Nero, D., Devenish, R.J. and Nagley, P. (1988) FEBS Lett. 236, 501–505.
11 Nagley, P., Farrell, L.B., Gearing, D.P., Nero, D., Meltzer, S. and Devenish, R.J. (1988) Proc. Natl. Acad. Sci. USA 85, 2091–2095.
12 Hadikusumo, R.G., Hertzog, P. and Marzuki, S. (1984) Biochim. Biophys. Acta 765, 257–267.
13 Grasso, D.G., Nero, D., Law, R.H.P., Devenish, R.J. and Nagley, P. (1991) Eur. J. Biochem. 199, 203–209.
14 Law, R.H.P., Devenish, R.J. and Nagley, P. (1990) Eur. J. Biochem. 188, 421–429.
15 Nero, D., Ekkel, S.M., Wang, L., Grasso, D.G. and Nagley, P. (1990) FEBS Lett. 270, 62–66.
16 Galanis, M., Devenish, R.J. and Nagley, P. (1991) FEBS Lett. 282, 425–430.
17 Devenish, R.J., Papakonstantinou, T., Galanis, M., Law, R.H.P., Linnane, A.W. and Nagley, P. (1992) Ann. N.Y. Acad. Sci. 671, 403–414.
18 Devenish, R.J., Galanis, M., Papakonstantinou, T., Law, R.H.P., Grasso, D.G., Helfenbaum, L. and Nagley, P. (1992) in Adenine Nucleotides in Cellular Energy Transfer and Signal Transduction (Papa, S., Azzi, A. and Tager, J.M., eds.), pp. 1–12, Birkhauser, Basel.
19 Vieira, J. and Messing, J. (1982) Gene 19, 259–268.
20 Messing, J. (1983) Methods Enzymol. 101, 20–78.
21 Krieg, P.A. and Melton, D.A. (1984) Nucleic Acids Res. 12, 7057–7070.
22 Law, R.H.P. and Devenish, R.J. (1988) Biochem. Int. 17, 673–679.
23 Yannisch-Peron, C., Vieira, J. and Messing, J. (1985) Gene 33, 103–119.
24 Sambrook, J., Fritsch, E.F. and Maniatis, T. (1989) Molecular Cloning – A Laboratory Manual, 2nd Edn., Cold Spring Harbor Laboratory, Cold Spring Harbor.
25 Klebe, R.J., Harriss, J.V., Sharp, Z.D. and Douglas, M.G. (1983) Gene 25, 333–341.
26 Davis, R.W., Thomas, M., Cameron, J., St. John, T.P., Scherer, S. and Padgett, R.A. (1980) Methods Enzymol. 63, 404–411.
27 Sanger, F., Nicklen, S. and Coulson, A.R. (1977) Proc. Natl. Acad. Sci. USA 74, 5463–5467.
28 Schmidt, B., Wachter, E., Sebald, W. and Neupert, W. (1984) Eur. J. Biochem. 144, 581–588.
29 Galanis, M., Law, R.H.P., O'Keefe, L.M., Devenish, R.J. and Nagley, P. (1990) Biochem. Int. 22, 1059–1066.
30 Nagley, P., Devenish, R.J., Law, R.H.P., Maxwell, R.J., Nero, D. and Linnane, A.W. (1990) in Bioenergetics: Molecular Biology, Biochemistry and Pathology (Kim, C.H. and Ozawa, T., eds.), pp. 305–325, Plenum, New York.
31 Glick, B.S., Brandt, A., Cunningham, K., Muller, S., Hallberg, R.L. and Schatz, G. (1992) Cell 69, 809–822.
32 Velours, J. and Guerin, B. (1986) Biochem. Biophys. Res. Commun. 138, 78–86.
33 Cheng, M.Y., Hartl, F.-U., Martin J., Pollock, R.A., Kalousek, F., Neupert, W., Hallberg, E., Hallberg, R.L. and Horwich, A.L. (1989) Nature 377, 620–625.
34 Ostermann, J., Horwich, A.L., Neupert, W. and Hartl, F.-U. (1989) Nature 341, 125–130.
35 Craig, E.A., Kramer, J., Shilling, J., Werner-Washburne, M., Holmes, S., Kosic-Smithers, J. and Nicolet, C.M. (1989) Mol. Cell. Biol. 9, 3000–3008.
36 Ackermann, S.H. and Tzagoloff, A. (1990) J. Biol. Chem. 265, 9952–9959.
37 Orian, J.M., Hadikusumo, R.G., Marzuki, S. and Linnane, A.W. (1984) J. Bioenerg. Biomembr. 16, 561–581.